Effects of alloying elements on the Snoek-type relaxation in Ti–Nb–X–O alloys (X = Al, Sn, Cr, and Mn)

H. Lu[a], C.X. Li[b], F.X. Yin[b], Q.F. Fang[a,*], O. Umezawa[c]

[a] *Key Laboratory of Materials Physics, Institute of Solid State Physics, Hefei 230031, China*
[b] *Exploratory Materials Research Laboratory for Reliability and Safety, National Institute for Materials Science, Tsukuba 305-0047, Japan*
[c] *Faculty of Engineering, Yokohama National University, Yokohama 240-8501, Japan*

ABSTRACT

The effect of alloying elements on the oxygen Snoek-type relaxation in the Ti–24Nb–X–1.7O alloys (X = 1Al, 2Al, 1Sn, 2Sn, 2Cr, 2Mn) was investigated in order to develop high damping materials based on point defect relaxation process. The relaxation strength of the Ti–Nb–Al–O and Ti–Nb–Sn–O alloys is the highest while that of the Ti–Nb–Mn–O and Ti–Nb–Cr–O alloys is the lowest. The dipole shape factor ($\delta\lambda$) and critical temperature T_c, which are intrinsic to the Snoek-type relaxation, were figured out and analyzed in terms of the d-orbital energy level (Md) for each alloy based on the measured damping peak. With the decreasing Md, the $\delta\lambda$ increases and saturates at last when the Md decreases to a certain value (about 2.435 eV), while the critical temperature T_c decreases linearly. The parameter Md can be taken as a key parameter in designing high damping β-Ti alloys, that is, to design an intermediate value of Md at which the values of both $\delta\lambda$ and T_c are as high as possible.

© 2012 Elsevier B.V. All rights reserved.

1. Introduction

High performance damping materials are nowadays receiving more and more attention owing to their wide applications in passive damping components to eliminate noise, to reduce mechanical vibration, and to protect buildings against earthquake, etc. Although the two or multiphase composites are believed to be a good candidate of high performance high-damping materials [1,2], the high-damping metals and alloys are still attractive in some applications. The damping mechanisms exploited in this kind of materials are dominantly the stress-induced movement of dislocation and planar defects. In the case of high concentration however, point defects can be also used as the main damping source [3]. For example, the Snoek-type relaxation damping mechanism has been applied to the design of high damping alloys such as the Ti–Nb–O alloys [4] and Ti–Mo–O alloys [5].

The Snoek-type relaxation is referred to the stress-induced reorientation process of the interstitial atoms in the body-centered cubic (bcc) substitutional alloys. Owing to the interactions among the substitutional atoms and interstitial atoms in the bcc alloys, the phenomena of Snoek-type relaxation are much more complex than the Snoek relaxation in pure bcc crystals. For example, the relaxation strength of the Snoek-type relaxation is dependent not only on the asymmetrical lattice distortion induced by the interstitial atoms, which can be described by the dipole shape factor $\delta\lambda = |\lambda_1 - \lambda_2|$, where λ_1 and λ_2 are the two principal values of the λ-tensor, but also on the so called self-induced ordering temperature, T_c [6]. Up to now however, most of the related researches were focused on the relaxation kinetics affected by the interactions [7], while rare work was conducted on the variation of $\delta\lambda$ and T_c. Although the $\delta\lambda$ values for interstitial atoms in bcc metals were calculated and measured [6], the $\delta\lambda$ for interstitial atoms in the bcc substitutional alloys rarely appears in the literatures, except for Ti–Nb–O alloys [8,9], which were designed as a kind of high-damping alloys [4].

The dipole shape factor $\delta\lambda$ relates closely not only to the properties of interstitial atoms but also to the alloy properties such as lattice constant and interatomic bonds or electronic states [10]. The self-induced ordering temperature T_c, which reflects the strength of the interaction between interstitial atoms mediated by the matrix or substitutional atoms, is strongly correlated with the interatomic bonds or electronic states. Therefore, addition of different types and amounts of alloying elements will strongly affect the values of $\delta\lambda$ and T_c, and in turn affect the Snoek-type relaxation. The understanding of the mechanism of such influences would be helpful in order to explore new type of high-damping alloys based on the Snoek-type relaxation.

In the present work, the influence of the alloying elements on the Snoek-type relaxation in the β-Ti–Nb alloys was investigated by adding 1–2 at% substitutional elements of Al, Sn, Cr, and Mn into the matrix alloy Ti–24Nb–1.7O, respectively. The $\delta\lambda$ and T_c of the Snoek-type relaxation were deduced from the measured

* Corresponding author. Tel.: +86 551 5591459; fax: +86 551 5591434.
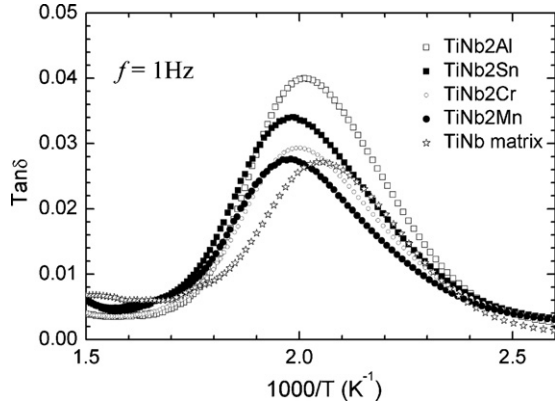*E-mail address:* qffang@issp.ac.cn (Q.F. Fang).

Fig. 1. Temperature-dependent damping capacity of Ti–24Nb–2X–O (X = Al, Sn, Cr, Mn) alloys and Ti–Nb–O matrix alloy at 1 Hz.

Fig. 2. Temperature-dependent damping capacity of a Ti–Nb–2Al–O alloy at different frequencies.

Snoek-type peak with the variable temperature and their relation with the lattice constant and the electronic property parameters was discussed.

2. Experimental procedures

Table 1 shows the nominal chemical compositions of the alloys studied in this work. The ingots of the Ti–24 at% Nb–1.7 at% O matrix alloy and Ti–Nb–X–O (X = Al, Sn, Cr, Mn) alloys were prepared in an argon-levitation melting furnace with a cold crucible. TiO_2 powder was added after the remelting of the ingots to obtain the desired Ti–Nb–X–O alloys with the same oxygen concentrations. Oxygen concentrations of the ingots were analyzed with infrared absorption method of the molten alloys. The samples were then cut into the dimensions of 1 mm thickness × 10 mm width × 60 mm length for the damping measurement.

The damping measurement was performed on a dynamic mechanical analyzer (DMA 2980, TA Instruments, Inc.) in the dual cantilever bending vibration mode. The strain amplitude was 3×10^{-4}. The vibration frequencies applied were 0.4, 1.0, 2.0, 4.0 and 10.0 Hz. Damping capacities at various vibration frequencies were measured at variable temperature with a heating rate of 2 K/min. The microstructures and textures of the Ti–Nb–X–O alloys were analyzed with the orientation imaging microscopy (OIM) system of TSL Inc., equipped on a LEO-1550 scanning electron microscope. The grain size distributions were deduced from the OIM images. The lattice constants of the Ti–Nb–X–O alloys at room temperatures were determined by the D8 Discover with GADDS Multipurpose X-ray Diffractometer (Bruker AXS) with Co Kα radiation and listed in Table 1.

3. Results and discussion

3.1. Damping behaviors of the Ti–Nb–X–O alloys

Fig. 1 shows the temperature-dependent damping capacities of the Ti–24Nb–2X–O (X = Al, Sn, Cr, Mn) alloys and the Ti–Nb–O matrix alloy at 1 Hz. In all alloys a prominent peak appears around 500 K. The Ti–Nb–Al–O alloy exhibits the highest value of tan δ (damping capacity), sequentially followed by the Ti–Nb–Sn–O, Ti–Nb–Cr–O, and Ti–Nb–Mn–O alloys, while the Ti–Nb–O matrix alloy exhibits the lowest value of tan δ. For each Ti–Nb–X–O alloy, the damping peak shifts toward higher temperature and decreases in height when the vibration frequency increases, as shown in Fig. 2 for the Ti–Nb–2Al–O alloy as an example. It is clear that this peak is the Snoek-type peak resulted from the stress induced re-orientation of oxygen in the Ti–Nb–X–O alloys. From the peak shift
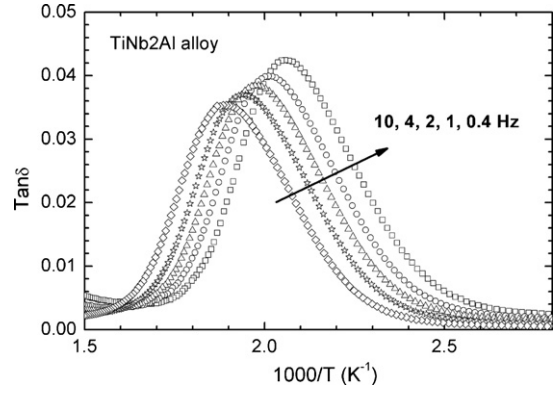
with frequency, the activation energy in the range of 1.5–1.8 eV can be deduced according to the Arrhenius relation. Young's modulus also varies apparently at peak position (not shown in Figs. 1 and 2 for clarity). These parameters as well as the peak temperature and peak height of the Snoek-type relaxations of these alloys are listed in Table 2.

3.2. Dipole shape factor and critical temperature of the Ti–Nb–X–O alloys

Considering the interaction between the interstitial solute atoms the relaxation strength of the Snoek-type peak can be expressed as follows [11]:

$$\Delta = \frac{2}{9} \cdot \frac{v_0 C_0}{k(T - T_c)} (\lambda_1 - \lambda_2)^2 \cdot E(\Gamma)(1 - 3\Gamma) \qquad (2)$$

with

$$\Gamma = \cos^2 \alpha \cos^2 \beta + \cos^2 \beta \cos^2 \gamma + \cos^2 \alpha \cos^2 \gamma \qquad (3)$$

where C_0 is the mole fraction of interstitial solute atoms, v_0 is the atomic volume of the host crystal, k is the Boltzmann constant, E is the elastic modulus, λ_1 and λ_2 are the two principal values of the λ-tensor, Γ is the orientation parameter of the crystal corresponding to the flexural oscillation stressing direction as defined in (3) where α, β, γ are the angles between the longitudinal stress axis and the cubic axes. The dipole shape factor δλ ($\delta\lambda = |\lambda_1 - \lambda_2|$) characterizes the tetragonal strain in bcc metals caused by the interstitial solutes. T_c has the significance of a critical temperature for self-induced ordering, and it implies the existence of an interaction between the interstitial solute atoms. In our case, the crystalline grain is randomly orientated and one can take Γ as 0.2. The values of C_0, v_0, and E can be taken as the oxygen content and values calculated from the lattice constant listed in Table 1, and Young's modulus at peak temperature listed in Table 2, respectively, depending upon the alloys composition.

The relaxation peak shown in Figs. 1 and 2 is broader than the standard Debye peak, indicating a distribution in the relaxation time. In this case, the relaxation strength Δ cannot be calculated directly by doubling the peak height, instead by integrating the internal friction (Q^{-1}) with respect to the $1/T$, that is, $\Delta = 0.276 \times (H/k) \int Q^{-1} d(1/T)$. The relaxation strength of the Snoek-type peaks was evaluated in this way and its reciprocal was drawn as a function of the peak temperature (T_p). As shown in Fig. 3, there is a linear relationship between $1/\Delta$ and T_p for all the alloys. From the slope and the intercept of these lines the dipole shape factor δλ and critical temperature T_c of the Snoek-type peak in these alloys can be deduced according to Eqs. (2) and (3) and are listed in Table 2. It can be seen from Table 2 that the Ti–Nb–Mn–O alloy has

Table 1
Nominal chemical compositions, lattice constants, and d-orbital energy (Md) of the Ti–Nb–X–O (X = Al, Sn, Cr, Mn) alloys.

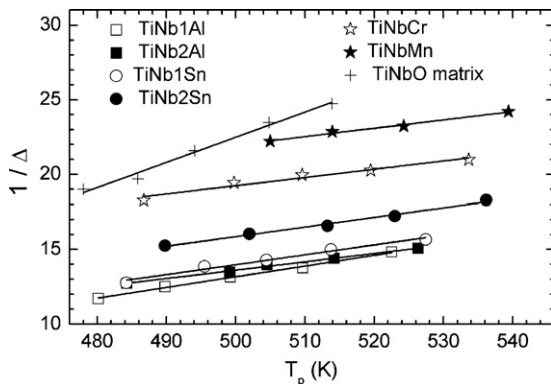| Ti–Nb–X	Nb wt% (at%)	X wt% (at%)	O wt% (at%)	Lattice constant (nm)	Md (eV)
Ti–Nb	39.0 (24.5)	0	0.47 (1.7)	0.3290	2.441
Ti–Nb–1Al	40.1 (25.2)	0.46 (1.0)	0.48 (1.7)	0.3286	2.439
Ti–Nb–2Al	39.4 (24.6)	0.93 (2.0)	0.45 (1.6)	0.3284	2.436
Ti–Nb–1Sn	40.4 (26.0)	2.02 (1.0)	0.48 (1.8)	0.3288	2.437
Ti–Nb–2Sn	35.3 (22.3)	3.38 (1.7)	0.44 (1.6)	0.3288	2.436
Ti–Nb–2Cr	38.7 (24.3)	1.80 (2.0)	0.46 (1.7)	0.3271	2.421
Ti–Nb–2Mn	38.8 (24.4)	1.59 (1.7)	0.45 (1.6)	0.3273	2.420

Table 2
Parameters of the Snoek-type relaxation (after subtracting the background) of the Ti–Nb–X–O alloys at 1 Hz: Young's modulus (E) at peak temperature (T_p), peak height ($\tan \delta_{max}$), activation energy (H), dipole shape factor ($\delta\lambda$), and the critical temperature (T_c).

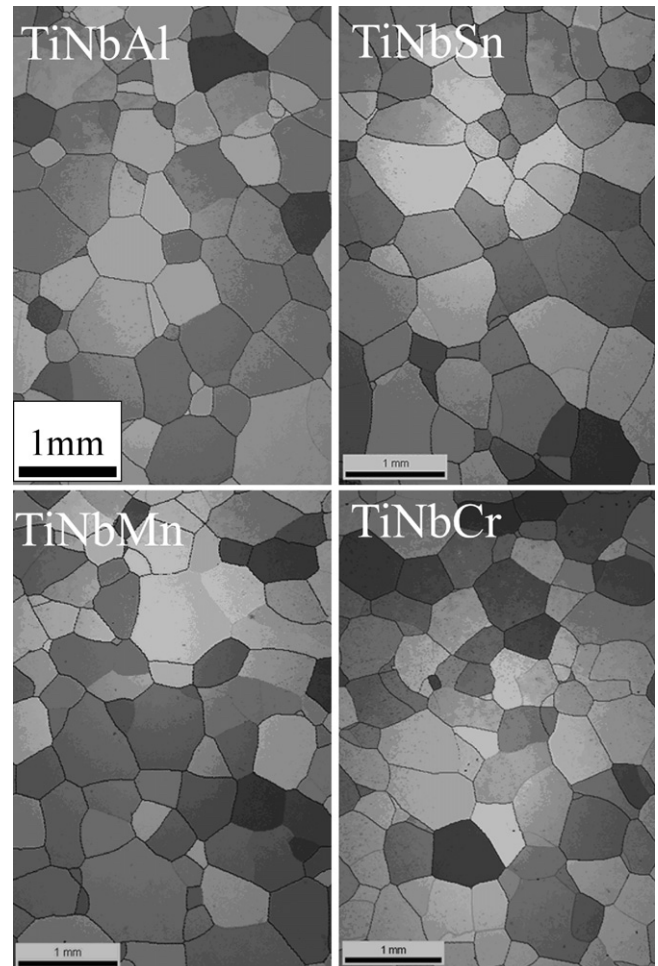| Ti–Nb–X	E (GPa)	T_p	H (eV)	$\tan \delta_{max}$ (10^{-2})	$\delta\lambda$	T_c (K)
Ti–Nb	60.30	486	1.79	2.58	0.225	366
Ti–Nb–1Al	64.37	490	1.64	4.09	0.329	316
Ti–Nb–2Al	61.63	499	1.61	3.80	0.395	256
Ti–Nb–1Sn	59.85	496	1.62	3.71	0.352	289
Ti–Nb–2Sn	60.46	502	1.60	3.04	0.374	252
Ti–Nb–2Cr	61.52	500	1.54	2.70	0.395	151
Ti–Nb–2Mn	60.09	505	1.52	2.44	0.400	108

the highest $\delta\lambda$ (0.4) and the lowest T_c (108 K) while the Ti–Nb–O matrix alloy has the lowest $\delta\lambda$ (0.225) and the highest T_c (366 K). These values of $\delta\lambda$ are comparable with the $\delta\lambda$ value reported in [8,9], but smaller than those of the bcc metals, which are higher than 0.5 [6]. The dipole shape factor $\delta\lambda$ and the critical temperature T_c of the Snoek-type relaxation peak depend on the grain size and the alloying elements to some extent [6]. The grain size of the present Ti–Nb–X–O (X = Al, Sn, Cr, Mn) polycrystals is similar (about 400 μm), as shown in Fig. 4. Therefore the effects of grain size on the $\delta\lambda$ can be ignored in this case and the variation of $\delta\lambda$ and the critical temperature T_c is mainly owing to the alloying elements, the effect of which will be discussed in the following sections.

It was reported that the dipole shape factor increases with the increasing difference between the size of the interstitial solute and the size of the octahedral interstice (generally, the size of the interstice is smaller than that of the interstitial solute), and decreases with the strengthening of the chemical interaction between the interstitial atoms and the host metal atoms [6]. Since the lattice constant is proportional to the size of the octahedral interstice, the relationship of the dipole shape factor $\delta\lambda$ with respect to the lattice constant of the Ti–Nb–X–O (X = Al, Sn, Cr, Mn) alloys was checked and shown in Fig. 5, where the data of matrix alloy Ti–Nb–O was also shown. Indeed the $\delta\lambda$ increases with the decreasing lattice constant and saturates at last when the lattice constant decreases to a certain value (about 0.3285 nm). The former is due to the decrease of the octahedral interstice. However, when the lattice constant decreases

to a certain value, the O atoms would adjust their sizes (and the octahedral interstice too) by transferring their charges with the neighboring metal atoms, and maintain a proper amount of distortion. This phenomenon was also reported in Fe–C and Fe–N by Morinaga et al. [12], where the C as well as N atoms tends to adjust

Fig. 4. Orientation imaging microscopy (OIM) images and the grain size distributions deduced from the OIM images.

Fig. 3. Linear relation between $1/\Delta$ and the peak temperature T_p at various frequencies of Ti–Nb–X–O (X = Al, Sn, Cr, Mn) alloys.

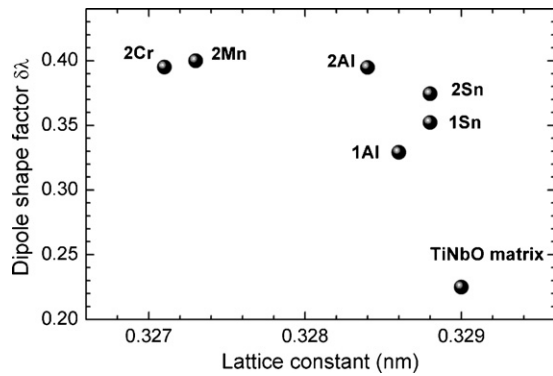**Fig. 5.** Variation of the dipole shape factor with respect to the lattice constant of Ti–Nb–X–O (X = Al, Sn, Cr, Mn) alloys.

Fig. 7. Relationship between the critical temperature T_c and Md for the Ti–Nb–X–O (X = Al, Sn, Cr, Mn) alloys.

their atomic sizes by transferring their charges with the neighboring Fe atoms, in order to obtain the most preferable state in the size under the proper amount of distortion.

The alloying elements not only change the lattice constant, but also affect the bonding state between the matrix atoms as well as between the interstitial and matrix atoms. To describe such bonding state, the parameter Md is a good choice. The parameter Md describes the d-orbital energy level, which correlates with the electro-negativity and the metallic radius of the elements. Md plays a dominant role when considering the alloying behaviors of metal alloys. For example, Morinaga et al. have investigated the electronic structure of titanium alloys [13], aluminum alloys [14], nickel-based superalloys [15], and high Cr ferritic steels [16]. Furthermore, this method was widely used in the design of titanium alloys [17–19]. Kurihara et al. [20] demonstrated that the d-orbital energy (Md) of the transition metal exhibited good correlations with the maximum solid solubility (MSS) of the transition metals in the nuclear materials.

The d-orbital energy (Md) for each alloy is calculated according to [18] and listed in Table 1. Since the parameter Md characterizes the interactions (between interstitial atoms and matrix atoms or other interstitial atoms) in the Ti alloys, it would be helpful to plot the dipole shape factor δλ as a function of Md to investigate the dependence of δλ on the atomic interactions. Fig. 6 shows the variation of the dipole shape factor δλ with respect to Md. It can be seen that the δλ increases with the decreasing Md and saturates at last when the Md decreases to a certain value (about 2.435 eV). This variation trend of δλ with Md is similar to that of δλ with the lattice constant, illustrating that the Md can characterizes the metallic radius of the elements in one aspect. Therefore, a higher value of
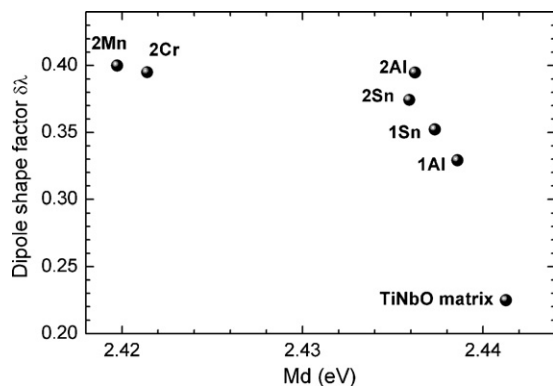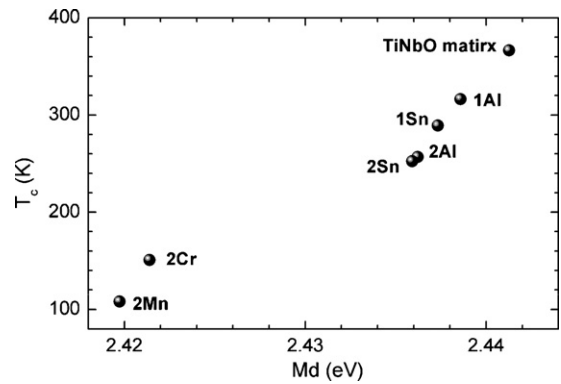
δλ can be obtained by adding alloying elements if these elements could decrease the lattice constant or the d-orbital energy Md.

In the other side, the critical temperature T_c depends upon the interaction strength between the interstitial atoms (here oxygen atoms). Since the interstitial atoms separate far away from each other at the content of 1.7 at%, the interaction between the interstitial atoms would be mediated by the interaction between the interstitial atoms and the matrix atoms. In this sense, the critical temperature T_c would be closely correlated with the d-orbital energy Md which characterizes the interaction of matrix atoms. Fig. 7 presents the T_c as a function of Md. It can be seen that the T_c increases almost linearly with Md.

From the view point of Md, one can understand the damping behavior of the Ti–Nb–X–O (X = Al, Sn, Cr, Mn) alloys and the Ti–Nb–O matrix alloy more clearly. For the Ti–Nb–Mn–O and Ti–Nb–Cr–O alloys with small Md, although the δλ is high but the T_c is small, which results in small relaxation strength according to Eq. (2). The Ti–Nb–O matrix alloy with large Md has the highest T_c but its δλ is the smallest, therefore its damping capacity is also low. For the Ti–Nb–Al–O and Ti–Nb–Sn–O alloys with intermediate Md, the value of δλ is high and the T_c is also high enough, so that the damping capacity is the highest. Therefore, the parameter Md is a key parameter in designing high damping β-Ti alloys by adding alloying elements, that is, to design an intermediate value of Md at which the values of both δλ and T_c are as high as possible.

4. Conclusion

In this paper, the damping behavior of Ti–Nb–X–O (X = Al, Sn, Cr, Mn) alloys was investigated in comparison with the matrix alloy Ti–Nb–O. The effects of alloying elements on the relaxation strength were analyzed in terms of the d-orbital energy Md. The main results can be summarized as follows:

(1) In the Ti–Nb–X–O (X = Al, Sn, Cr, Mn) alloys, a prominent Snoek-type relaxation peak associated with the stress induced re-orientation of interstitial oxygen atoms was observed. The peak height (damping capacity) of the Ti–Nb–Al–O and Ti–Nb–Sn–O alloys is the highest while that of the Ti–Nb–Mn–O and Ti–Nb–Cr–O alloys is the lowest.
(2) The effect of alloying elements on the relaxation strength of Snoek-type relaxation peak is manifested through their influence on the dipole shape factors (δλ) and the critical temperature T_c, which can be well elucidated in terms of the d-orbital energy Md.
(3) The dipole shape factors δλ increase with the decreasing Md and saturate at last when the Md decreases to a certain value

Fig. 6. Relationship between the dipole shape factor and Md for the Ti–Nb–X–O (X = Al, Sn, Cr, Mn) alloys.

(about 2.435 eV), while the critical temperature T_c increases linearly with Md.

(4) It was suggested that the Md can be used as a key parameter in designing high damping β-Ti alloys.

References

[1] H. Lu, X. Wang, T. Zhang, Z. Cheng, Q. Fang, Materials 2 (2009) 958–977.
[2] W.G. Wang, C. Li, Y.L. Li, X.P. Wang, Q.F. Fang, Mater. Sci. Eng. A 518 (2009) 190–193.
[3] X.P. Wang, W.G. Wang, Y.X. Gao, T. Zhang, Q.F. Fang, Mater. Sci. Eng. A 521–522 (2009) 87–89.
[4] F. Yin, S. Iwasaki, D. Ping, K. Nagai, Adv. Mater. 18 (2006) 1541–1544.
[5] H. Lu, C. Li, F. Yin, Q. Fang, O. Umezawa, Mater. Sci. Eng. A 528 (2011) 3358–3366.
[6] M.S. Blanter, I.S. Golovin, H. Neuhäuser, H.-R. Sinning, Internal Friction in Metallic Materials – A handbook, Springer, Berlin, Heidelberg, 2007.
[7] H.R. Sinning, I.S. Golovin, A. Strahl, O.A. Sokolova, T. Sazonova, Mater. Sci. Eng. A 521–22 (2009) 63–66.
[8] F. Yin, L. Yu, D. Ping, S. Iwasaki, J. Appl. Phys. 104 (2008) 8.
[9] F. Yin, L. Yu, D. Ping, Mater. Sci. Eng. A 521–522 (2009) 372–375.
[10] T. Saito, T. Furuta, J.-H. Hwang, S. Kuramoto, K. Nishino, N. Suzuki, R. Chen, A. Yamada, K. Ito, Y. Seno, T. Nonaka, H. Ikehata, N. Nagasako, C. Iwamoto, Y. Ikuhara, T. Sakuma, Science 300 (2003) 464–467.
[11] A.S. Nowick, B.S. Berry, Anelastic Relaxation in Crystalline Solids, Academic Press, New York, 1972.
[12] M. Morinaga, N. Yukawa, H. Adachi, T. Mura, J. Phys. F: Met. Phys. 17 (1987) 2147–2162.
[13] M. Morinaga, N. Yukawa, H. Adachi, J. Iron Steel Inst. Jpn. 72 (1986) 555–562.
[14] M. Moringa, S. Nasu, H. Adachi, J. Saito, N. Yukawa, J. Phys.: Condens. Matter 3 (1991) 6817–6828.
[15] M. Morinaga, N. Yukawa, H. Adachi, J. Phys. Soc. Jpn. 53 (1984) 653–663.
[16] M. Morinaga, Y. Murata, H. Yukawa, in: S.G. Kang, T. Kobayashi (Eds.), Designing, Processing and Properties of Advanced Engineering Materials, Pts 1 and 2, 2004, pp. 37–42.
[17] D. Kuroda, M. Niinomi, M. Morinaga, Y. Kato, T. Yashiro, Mater. Sci. Eng. A 243 (1998) 244–249.
[18] M. Abdel-Hady, K. Hinoshita, M. Morinaga, Scripta Mater. 55 (2006) 477–480.
[19] R.J. Talling, R.J. Dashwood, M. Jackson, D. Dye, Scripta Mater. 60 (2009) 1000–1003.
[20] M. Kurihara, J. Onoe, M. Hirata, C. Suzuki, J. Alloys Compd. 509 (2011) 1152–1156.